



Published in final edited form as:

Cell Signal. 2012 March ; 24(3): 734–741. doi:10.1016/j.cellsig.2011.11.007.

HIV-associated Nephropathy : Role of AT₂R

Divya Salhan, Ankita Sagar, Dileep Kumar, Rungwasee Rattanavich, Partab Rai, Subani Maheshwari, Madhuri Adabala, Mohammad Husain, Guohua Ding, Ashwani Malhotra, Praveen N. Chander, and Pravin C. Singhal

Division of Kidney Diseases and Hypertension, North Shore-LIJ Health System, Great Neck, NY and Department of Pathology, New York Medical College, Valhalla, NY

Abstract

AT₁R has been reported to play an important role in the progression of HIV-associated nephropathy (HIVAN); however, the effect of AT₂R has not been studied. Age and sex matched control (FVB/N) and Tg26 mice aged 4, 8, and 16 weeks were studied for renal tissue expression of AT₁R and AT₂R (Protocol A). Renal tissue mRNA expression of AT₂R was lower in Tg26 mice when compared with control mice. In protocol B, Tg26 mice were treated with either saline, telmisartan (TEL, AT₁ blocker), PD123319 (PD, AT₂R blocker), or TEL + PD for two weeks. TEL-receiving Tg26 (TRTg) displayed less advanced glomerular and tubular lesions when compared with saline-receiving Tg26 (SRTg). TRTgs displayed enhanced renal tissue AT₂R expression when compared to SRTgs. Diminution of renal tissue AT₂R expression was associated with advanced renal lesions in SRTgs; whereas, upregulation of AT₂R expression in TRTgs was associated with attenuated renal lesions. PD-receiving Tg 26 mice (PDRTg) did not show any alteration in the course of HIVAN; whereas, PD + TEL-receiving Tg26 (PD-TRTg) showed worsening of renal lesions when compared to TRTgs. Interestingly, plasma as well as renal tissues of Tg26 mice displayed several fold higher concentration of Ang III, a ligand of AT₂R.

Ang II has been reported to play an important role in the progression of HIV-associated nephropathy (HIVAN) (1–3). Drugs which either blocked the AT₁R or inhibited the production of Ang II also slowed down the progression of HIVAN (1–3). On the other hand, infusion of Ang II in a mouse model of HIVAN accelerated the progression of renal lesions (4). Since use of AT₁ receptor blockers partially inhibited the progression of HIVAN, it was suggested that AT₁R activation contributing to the progression of HIVAN (3). Ang II exerts its effects via Ang II receptors (ATRs), AT₁R and AT₂R (5). Because AT₂R and AT₁R exert opposite effects (6–9), it is plausible that down regulation of AT₂R may have similar effects as of the activation of AT₁R in the pathogenesis of HIVAN; conversely, up-regulation of AT₂R may have effects similar to the blockade of AT₁R. However, the role of AT₂R in the pathogenesis of HIVAN has not been investigated to date. We hypothesize that in addition to AT₁R blockade, the upregulation of AT₂R (during AT₁R blockade) may contribute to the attenuation of the progression of HIVAN.

AT₂R is a member of the 7 trans-membrane spanning receptor family (10, 11). It shares 34% sequence homology to the AT₁R (7). It is expressed abundantly during embryogenesis, but

© 2011 Elsevier Inc. All rights reserved.

Address for correspondence: Pravin C. Singhal, M.D., Division of Kidney Diseases and Hypertension, 100 Community Drive, Great Neck, NY 11021, Tel. 516-465-3010, Fax 516-465-3011, psingahal@nshs.edu.

Publisher's Disclaimer: This is a PDF file of an unedited manuscript that has been accepted for publication. As a service to our customers we are providing this early version of the manuscript. The manuscript will undergo copyediting, typesetting, and review of the resulting proof before it is published in its final citable form. Please note that during the production process errors may be discovered which could affect the content, and all legal disclaimers that apply to the journal pertain.

levels decline during post-natal period (6). On that account, AT₂R was considered to be involved primarily in cellular growth and differentiation (12, 13). In adults, the AT₂R has been localized to the heart, kidney, adrenal gland, brain, uterus, pancreas, retina, skin, and both endothelial and vascular smooth muscle cells (VSMCs) of the vasculature (14–17); Interestingly, expression of AT₂R has also been reported to be increased in several cardiovascular injuries (18, 19).

Although both AT₁ and AT₂ receptors bind Ang II with nanomolar affinity, yet display different outcomes (20, 21). The AT₁R contributes to several pathological effects including proliferation, hypertension, coagulation, and inflammation (21). On the other hand, the AT₂R counteracts these effects of the AT₁R by enhancing apoptosis, hypotension, and anti-inflammatory events (20, 21). Several investigators had suggested that the AT₂R was constitutively active and capable of mediating downstream signaling without any requirement of Ang II binding (22, 23). This notion was based on the observations- direct correlation between apoptosis and levels of AT₂R protein expression in cultured fibroblasts, epithelial cells, and VSMCs (22). In addition, Ang II did not modulate the rate of apoptosis of up-regulated AT₂R expressing cells (24). Furthermore, modification of Ang II side chains, which modulated AT₁R function, had minimal effect on AT₂R function, suggesting that AT₂R was already in an active state (25).

Other metabolites of Ang II, including Ang III, Ang IV, and Ang (1–7) have also been demonstrated to carry biologic activities (26). Ang III plays an important role in brain and cardiovascular physiologic processes (26). Many of the effects originally attributed to Ang II, such as vasopressin release, are found to be in response to Ang III (27). Other investigators suggested that Ang III might be involved in several renal pathophysiologic processes (28–30). Ang III has been demonstrated to increase kidney cell expression of angiotensinogen, transforming growth factor- β , fibronectin, and monocyte chemoattractant protein-1 (MCP-1) (29, 30). Ang III binds predominantly to AT₂R and displays lower affinity for AT₁R (31). Interestingly, Ang III has 40% of the pressor activity of Ang II, but 100% of aldosterone producing activity. The half life of Ang III in the circulation is around 30 seconds, whereas in tissues it may be as long as 15–30 minutes. Prolonged half life of Ang III in tissues not only promotes its accumulation but also enhances its effectiveness.

In the present study, we have studied renal tissue expression of AT₂R receptors in a mouse model of HIVAN (Tg26) and control mice. Renal tissues in Tg26 mice showed attenuated expression of AT₂R when compared with renal tissues of control mice. Interestingly, blockade of AT₁R in Tg26 mice not only enhanced expression of AT₂R but also attenuated the progression of HIVAN. Thus, it appeared that enhanced AT₂R expression during AT₁R blockade may also be contributing to the attenuated progression of HIVAN. We have also examined the effect of AT₂R blockade alone as well as in combination with AT₁ blockade on the progression of HIVAN. In addition, we have measured plasma and renal tissue Ang III levels, a proposed ligand for AT₂R, in control and HIV-1 transgenic mice.

Material and Methods

HIV transgenic mice

We have used age and sex matched FVB/N (control) and Tg26 (on FVB/N background). Breeding pairs of FVB/N were obtained from Jackson Laboratories (Bar Harbor, ME). Breeding pairs to develop Tg26 colonies were kindly gifted by Prof. Paul E. Klotman M.D., President and CEO, Baylor College of Medicine, Houston, TX). The Tg26 transgenic animal has the proviral transgene, pNL4-3: d1443, which encodes all the HIV-1 genes except *gag* and *pol* and therefore the mice are noninfectious (32). Mice were housed in groups of 4 in a laminar-flow facility (Small Animal Facility, Long Island Jewish Medical Center, New

Hyde Park, NY). We are maintaining the colonies of these animals in our animal facility. For genotyping of these animals, tail tips were clipped, DNA was isolated and PCR studies were carried out using following primers for Tg26.

HIV-F 5' ACATGAGCAGTCAGTTCTGCCGCAGAC

HIV-R 3' CAAGGACTCTGATGCGCAGGTGTG

The Ethics Review Committee for Animal Experimentation of Long Island Jewish Medical Center approved the experimental protocol.

Experimental studies

Protocol A

Control (FVB/N) and Tg26 mice (n=4 for each group) aging 4, 8, 16 weeks were sacrificed and evaluated for renal tissue mRNA expression of AT₂R and renal histology.

Protocol B

Sixteen Tg26 mice aging 3 weeks in groups of four were anesthetized by inhalation anesthesia (isoflurane + oxygen). The Alzet minipumps (model # 2004, Durect Corp. Cupertino, CA) containing either saline or Telmisartan (AT₁R blocker, 300 µg/day), PD123319 (AT₂R blocker, 3 µg/day), telmisartan + PD123319 were implanted subcutaneously. Four age and sex matched FVBN mice-receiving saline through minipumps served as control for Tg26 mice receiving saline. After two weeks of infusion, animals were sacrificed and renal biomarkers were collected as described below.

At the end of the scheduled periods, the animals were anesthetized (by inhalation of isoflurane and oxygen) and sacrificed (by a massive intraperitoneal dose of sodium pentobarbital). After euthanization, both kidneys were excised; one was processed for histological and immunohistochemical studies while the other was used for RNA and protein extraction. Three-micrometer sections were prepared and stained with hematoxylin-eosin and periodic-acid Schiff. Blood pressure (systolic and diastolic) was measured by DOCA system (Kent Scientific Corp. CT) at the end of the experimental period. Proteinuria was measured by automated analyzer, which quantified the levels as low as 1.0 microgram/ml.

Renal Histology—Renal cortical sections were stained with hematoxyline and eosin and PAS. Renal histology was scored for both tubular and glomerular injury. Renal cortical sections were coded and examined under light microscopy. Twenty random fields (20X)/mouse were examined to score percentage of the involved glomeruli and tubules.

Immunohistochemical staining

The immunohistochemistry protocol used in the present study has been described previously (33). Briefly, the sections were de-paraffinized and antigen retrieval was accomplished by microwave heating for 10 minutes at maximum output in 10 mM citrate buffer (pH 6.0). The endogenous peroxidase activity was blocked with 0.3% hydrogen peroxide in methanol for 30 minutes at room temperature (RT). Sections were washed in phosphate buffered saline (PBS) thrice and incubated in blocking serum solution according to the primary antibody for 1 hour at RT. The primary antibody was applied in different dilutions: AT₁R (1:500, #2971, Cell Signaling) and AT₂R (mouse monoclonal, 1:1000, #7279, Santa Cruz) and then incubated overnight at 4°C in a humidifying chamber. Each of the sections were washed thrice with PBS and incubated in the appropriate secondary antibody at 1:250 dilutions at RT for 1 hour. After washing with PBS three times, sections were incubated in ABC reagent

(Vector Laboratories, Burlingame, CA) for 30 minutes. Sections were washed thrice in PBS and placed in VECTOR Nova RED substrate kit SK-4800 (Vector Laboratories, Burlingame, CA) followed by counterstaining with methyl green. The sections were then dehydrated and mounted with a xylene-free mounting media (Permount, Fisher Scientific Corporation, Fair Lawn, NJ). In all the batches of immunostaining, appropriate positive and negative controls were used. All the immune-stained slides were coded and blindly studied by two pathologists by a semiquantitative grading score.

Co-labeling of renal cortical sections

The kidneys were perfused in situ and then fixed with fresh 4% PFA and stored in 10% formalin. Subsequently, paraffin sections (4 μ m) were prepared and de-paraffinated in xylene and re-hydrated through graded alcohol concentrations. Epitope retrieval was carried out by heating the samples at 98° C for 2 hrs in Retrieveall-1 (Signet Laboratories, Inc). Subsequently, cooled samples were permeabilized with 0.1% triton X for 10 min. Section were blocked with 10% goat serum for 45 min at room temperature followed by incubated with AT1R antibody (MsmAb ab9391, abcam) and AT2R antibody (Rb pAb ab78747, abcam) over night followed by incubation with appropriate secondary antibody and mounting the sections under the coverslips.

Protein extraction and Western blotting

Renal cortical tissue were mixed with lysis buffer (1x PBS, pH 7.4, 0.1% SDS, 1% NP-40, 0.5% sodium deoxycholate, 1.0 mM sodium orthovanadate, 10 μ l of protease inhibitor cocktail, 100X (Calbiochem) per one ml of buffer, and 100 μ g/ml PMSF), homogenized with a dounce homogenizer and then incubated on ice for 30 min. The samples were subjected to centrifugation at 15,000g for 20 min at 4°C. The collected supernatant was evaluated for protein concentration as determined by a BCA kit (Pierce, Rockford, IL). The proteins, 20–40 μ g/lane, were separated by 10 or 12% sodium dodecyl sulfate-polyacrylamide gel electrophoresis and transferred onto a nitrocellulose membrane using a Bio-Rad Western blotting apparatus. After transfer, blots were stained with Ponceau S (Sigma, MO) to check for complete protein transfer and equal loading. The blots were blocked with 0.5% BSA and 0.1% TWEEN 20 in 1X PBS for 60 min at room temperature and then incubated with the AT1R (1:1000, Santa Cruz Biotechnology, CA) or AT2R (Santa Cruz) overnight at 4°C. A horseradish peroxidase-conjugated appropriate secondary antibody was applied for 1 hour at RT. The blots were then developed using a chemiluminescence detection kit (ECL, Amersham, Arlington Heights, IL) and exposed to Kodak X-OMAT AR film. To reassure equal loading of proteins, the blots were striped and reprobed for actin.

Reverse Transcription PCR Analysis

Control and experimental renal tissues were used to quantify mRNA expression. RNA was extracted using TRIZOL (Invitrogen corp.). For cDNA synthesis, 2 μ g of the total RNA was preincubated with 2 nmol of random hexamer (Invitrogen Corp) at 65°C for 5 min. Subsequently, 8ul of the reverse-transcription (RT) reaction mixture containing Cloned AMV RT, 0.5 mmol each of the mixed nucleotides, 0.01 mol dithiothreitol, and 1000 U/mL Rnasin (Invitrogen Corp) was incubated at 42°C for 50 min. For a negative control, a reaction mixture without RNA or reverse transcription (RT) was used. Samples were subsequently incubated at 85°C for 5 min to inactivate the RT.

Quantitative PCR was carried out in an ABI Prism 7900HT sequence detection system using the primer sequences as shown below:

AT₁R F GCACAATCGCCATAATTATCC

```

R   CACCTATGTAAGATCGCTTC
AT2R F TTATGGCTTCCACCTGAG
R   AAGGAAGTGCCAGGTCAATG

```

SYBR green was used as the detector and ROX as the passive reference gene. Results (means \pm S.D.) represent three animals as described in the legend. The data was analyzed using the Comparative C_T method ($\Delta\Delta^{CT}$ method). Differences in C_T are used to quantify relative amount of PCR target contained within each well. The data was expressed as relative mRNA expression in reference to control, normalized to quantity of RNA input by performing measurements on an endogenous reference gene, GAPDH.

Ang III ELISA

Ang III levels were determined in the renal tissue and plasma samples from age and sex matched control and Tg26 mice using commercial ELISA kits (Peninsula Laboratories, San Carlos, CA) as described by the manufacturer. Briefly, Ang III was extracted with 20 mM Tris buffer, Ph7.4 and partially purified and concentrated after filtering through Centricon Filters (MW cut off 10,000).

Statistical analysis

For comparison of mean values between two groups, the unpaired t test was used. Results are represented as means \pm SD. Statistical significance was defined as P<0.05.

Results

Growing control and Tg26 mice displayed a decrease in AT₂R

Total RNA was extracted from renal tissues of age and sex matched control (FVBN, 4 and 8 weeks old) and Tg26 (4 and 8 weeks old) mice. Renal tissue expression of AT₂R was determined by real time PCR studies. As shown in Fig. 1, renal tissue AT₂R expression diminished with age both in control (Fig 1A) and Tg26 mice (Fig. 1B).

Aging control and Tg26 mice showed diminution of both AT₁R and AT₂R

Total RNA from renal tissues of eight and 16 weeks old control (FVBN) and Tg26 mice was extracted. Renal tissue expression of AT₁R and AT₂R was assayed by real time PCR studies. As shown in Fig 2, Tg 26 mice showed lower renal tissue mRNA expression of AT₁R when compared to control mice at age 8 (Fig. 2A) and 16 (Fig. 2B) weeks. Similarly, Tg26 mice displayed significantly decreased expression of AT₂R at age 8 (Fig. 2C) and 16 (Fig. 2D) weeks when compared to respective control mice. However, decline in AT₂R expression was more prominent than of AT₁R expression.

Kidney cells displayed immunolabeling for AT₁R and AT₂R in Tg26

Both glomerular and tubular cells showed expression of AT₁R in Tg26 mice. However, control mice displayed predominantly AT₁R expression by tubular cells only. Representative microphotographs are shown in Fig. 3A. Tubular cells displayed moderate expression of AT₂R in control mice; whereas, tubular cells in Tg26 mice displayed minimal AT₂R expression (Fig. 3A).

To determine temporo- spatial relationship between AT₁R and AT₂R in glomerular and tubular cells, renal cortical sections were co-labeled for AT₁R and AT₂R. As shown in Fig. 3B, some glomerular and tubular cells displayed expression of both AT₁R and AT₂R (merged); whereas other cells displayed expression of either AT₁R or AT₂R. Renal cells in Tg26 mice displayed enhanced labeling for AT₁R and diminished labeling for AT₂R.

To determine quantitative expression of AT₁R and AT₂R by renal tissues in FVBN and Tg26 mice, renal tissue lysates were electrophoresed and then labeled for AT₁R, AT₂R and actin. Representative gels are shown in Fig. 3C. Renal tissues of Tg26 mice showed enhanced ($P<0.01$) AT₁R expression (Fig. 3D) and diminished ($P<0.05$) AT₂R expression (3E).

AT₁R blockade not only attenuated progression of HIVAN but also increased renal tissue AT₂R expression

Tg26 mice receiving AT₁R blocker (telmisartan, TRTg) displayed attenuated glomerular and tubular lesions when compared with saline receiving Tg26 mice (SRTg). Representative microphotographs showing glomerular and tubular lesions in a TRTg and a SRTg are shown in Fig. 4. Cumulative data displaying percent of glomeruli developing sclerosis and microcysts are shown in Fig 5.

To determine the effect of AT₁R blockade on blood pressure of Tg26 mice, blood pressure was recorded in SRTgs, TRTgs and TRTgs receiving PD123319. AT₁ blockade in TRTgs and TRTg receiving PD123319 was associated with significant decrease both in systolic and diastolic blood pressure levels (Table 1).

To determine whether AT₁R blocker-mediated attenuation of renal lesions was the sole outcome of AT₁R blockade or was also contributed partly by the upregulation of AT₂R, we studied renal tissue expression of AT₂R in TRTgs by immunohistochemical studies. As shown in Fig. 6, renal tissue of TRTg displayed increased AT₂R expression when compared with SRTg.

To further confirm the occurrence of enhanced renal tissue expression of AT₂R in TRTgs, we carried out immunoblotting studies in renal tissues of TRTgs (n=3) and SRTgs (n=3). Representative gels of SRTgs and TRTgs are shown in Fig. 7A. Cumulative data in the form of bar diagram is shown in Fig. 7B. All renal tissue samples from TRTgs showed several fold increase in expression of AT₂R when compared with SRTg (Fig. 7B).

Blockade of AT₂R in TRTgs accelerated the progression of renal lesions

We hypothesized that enhanced expression of AT₂R might have contributed to slowed progression of HIVAN in TRTgs. To test our hypothesis, TRTgs were administered either normal saline or AT₂R blocker for two weeks. Blockade of AT₂R in TRTgs accelerated the progression of both glomerular and tubular lesions. Representative microphotographs of renal cortical sections from a TRTg mouse and a mouse receiving TRTg + AT₂R blocker are shown in Fig. 4. Cumulative data of severity of renal lesions in TRTgs and TRTg + AT₂R blocker are show in Fig. 5. These findings indicated that enhanced renal tissue expression of AT₂R has also contributed to the attenuation of the progression of renal lesions in TRTgs.

Tg26 mice showed enhanced plasma and renal tissue levels of Ang III

Ang III is a metabolic product of Ang II and has been considered to act as a ligand for AT₂R (31). To determine the status of plasma Ang III and renal tissue Ang III, proteins were extracted from plasma and renal tissue samples of age and sex matched four control (FVBN) and four Tg26 mice. Plasma and renal tissue concentration was assayed using Ang III ELISA kits. As shown in Fig. 8, mean plasma concentration of Ang III in Tg 26 mice was 28 fold higher when compared with control mice (Fig. 8A). Similarly, mean renal tissue concentration of Ang III in Tg26 was 3.8 fold higher when compared with control mice (Fig. 8B).

Discussion

In the present study, aging Tg26 mice showed attenuated renal tissue expression of AT₂R when compared with control mice. Although AT₁R expression in Tg26 mice was also diminished in aging mice, but diminution of renal tissue AT₂R expression was more pronounced than the AT₁R when compared to control mice. On the other hand, both plasma and renal tissue concentrations of Ang III were higher in Tg26 mice when compared to control mice. Since Tg26 mice displayed attenuated expression of AT₂R despite overt renal injury it appeared that HIV-1 had compromised cellular response- AT₂R expression in response to an ongoing injury. Interestingly, telmisartan-receiving Tg26 mice not only showed enhanced expression of AT₂R but also displayed attenuated progression of HIVAN. On the other hand, administration of AT₂R blocker in telmisartan-receiving mice accelerated the progression of HIVAN. These findings indicated that upregulation of AT₂R in telmisartan-receiving Tg26 mice might have partially contributed to the attenuated progression of renal lesions.

The AT₁R has been reported to function as a dimer; however, both homodimers and heterodimers have also been reported (34). AT₂R has been demonstrated to function as an antagonist of the AT₁R (35). In these studies, AT₂R bound directly to the AT₁R, and its AT₁R antagonistic property was independent of downstream signaling. It was speculated that AT₁R could not bind with other activating G proteins coupled receptors (GPCRs) and to G proteins because AT₂R altered AT₁R conformation, which prevented its self dimerization.

Several investigators demonstrated that AT₂R was functional in the absence of ligand binding (22, 24, 36). AT₂R over-expressing fibroblasts, epithelial cells and VSMCs not only displayed the activation of p38 MAPK and caspase-3 signaling but also induction of apoptosis (22); interestingly, the degree of apoptosis correlated to AT₂R expression rather than to the levels of Ang II or AT₁ receptor blockade (22); moreover, AT₂R over-expressing cultured VSMCs showed down-regulation of AT₁R in a ligand-dependent manner (24). These investigators demonstrated the role of bradykinin/nitric oxide signaling for the reduction of AT₁R expression in AT₂R over-expressing cells (24); interestingly, VSMC down regulation of AT₁R in WKY was also associated with diminished DNA synthesis both under basal and Ang II-stimulated states (36).

Multiple studies demonstrated that Ang II levels modulate only AT₁R expression but not the expression of AT₂R (37–39). AT₁R and AT₂R expressing human embryonic kidney 293 cells neither displayed any alteration of AT₂R surface binding in the presence of higher Ang II levels (38) nor internalization of AT₂R after agonist exposure (39); whereas, AT₁R was rapidly internalized (37, 39). Thus, it appears that AT₂R effects may remain un-interrupted during the sustained higher Ang II levels.

Usually AT₂R expression is higher than that of AT₁R expression in the fetal kidney (40, 41). However, the relative proportion of these receptors reverses during post-natal and the later time periods. AT₂R are barely detectable in adult kidney. AT₂R mRNA and protein are uniformly expressed in tubules and vascular segments but there is a significant variability in their expression in glomeruli (42–44). These discrepancies between studies may be related to species differences (45, 46). Observations on age related diminished renal tissue AT₂R expression in the present study, are consistent with the findings of other investigators.

In the present study, attenuated progression of HIVAN in telmisartan-receiving Tg26, indicated the activation of RAS in HIVAN. These findings are consistent with other investigators' observations (3). Interestingly, Tg26 mice also displayed a decrease in renal tissue mRNA expression of AT₂R. Contrary to the observations in the present study, AT₂R

had been reported to be invariably up-regulated in the models of overt renal damage, such as induced by renal ablation and subtotal nephrectomy, or kidney damage caused by protein overload (44, 47–51). In these studies, ex vivo analysis indicated that increased AT₂R expression was associated with enhanced renal vasodilatation in perfused kidneys (48); in addition, persistent proteinuria was associated with enhanced tubular cell apoptosis (50). Similar to AT₁R blockade, blockade of AT₂R with PD123319 was associated with diminution of proteinuria (47). These results suggested that both AT₁R and AT₂R provided reno-protection in the subtotal nephrectomy model (47); however, recent data using the same model disputes those findings (51–53). There was a time-dependent increase in AT₂R expression in a renal ablation model (51). In this study, blockade of AT₂R by PD123319 not only exacerbated renal ischemia/damage but also caused a marked increase in blood pressure (51). Moreover, mice treated with PD123319 as well as AT₂R deleted mice displayed accelerated renal fibrosis (52, 53). Similarly, vascular over-expression of AT₂R ameliorated glomerular injury in the mouse remnant kidney model (49). Thus, majority of studies indicate that AT₂R provides renal protection. However, in the present study, neither renal injury increased renal tissue AT₂R expression nor PD123319 administration modulated the course of HIVAN in Tg26 mice. We speculate that PD123319 did not alter the course of HIVAN because of the attenuated renal tissue expression AT₂R in Tg26 mice. On the other hand, Tg26 mice-receiving telmisartan displayed enhanced renal tissue expression of AT₂R; therefore, administration of PD123319 in these animals accelerated the progression of HIVAN.

In the present study, both plasma and renal tissue levels of Ang III were higher in Tg26 mice. Ang III has been reported to act as a ligand for the activation of AT₂R (31). The role of Ang III in the development of kidney disease models in general and HIVAN in particular has not been investigated to date. In the present study, Tg26 mice displayed several fold higher plasma and renal tissue levels of Ang III. Since Tg26 mice showed attenuated expression of AT₂R, it appears that enhanced levels of Ang III may be a compensatory approach. However, it will be interesting to evaluate the direct role of Ang III in the development of HIVAN in future studies.

We conclude that both up-regulation and or blockade of AT₂R in telmisartan-receiving TG26 mice contributed to the altered course of HIVAN. The present study provides an insight into the role of AT₂R in the progression of HIVAN.

Acknowledgments

This work was supported by grant RO1DK084910 and RO1 DK083931 (PCS) from National Institutes of Health, Bethesda, MD. We are grateful to Prof. Paul E. Klotman, President and CEO, Baylor college of Medicine, Houston, Texas, for providing a breeding pair of Tg26 mice. This work was presented at the 41st Annual Meeting of the American Society of Nephrology on November 18th, at the Denever Convention Center, Denever, CO.

References

1. Burns GC, Paul SK, Toth IR, Sivak SL. Effect of angiotensin-converting enzyme inhibition in HIV-associated nephropathy. *J Am Soc Nephrol.* 1997; 8:1140–1146. [PubMed: 9219164]
2. Bird JE, Durham SK, Giancarli, Gitliz PH, Pandya DG, Dambach DM, Mozes MM, Kopp JB. Captopril prevents nephropathy in HIV-transgenic mice. *J Am Soc Nephrol.* 1998; 9:1441–1447. [PubMed: 9697666]
3. Hiramatsu N, Hiromura K, Shigehara T, Kuroiwa T, Ideura H, Sakurai N, Takeuchi S, Tomioka M, Ikeuchi H, Kaneko Y, Ueki K, Kopp JB, Nojima Y. Angiotensin II type 1 receptor blockade inhibits the development and progression of HIV-associated nephropathy in a mouse model. *J Am Soc Nephrol.* 2007; 18:515–27. [PubMed: 17229913]

4. Ideura H, Hiromura K, Hiramatsu N, Shigehara T, Takeuchi S, Tomioka M, Sakairi T, Yamashita S, Maeshima A, Kaneko Y, Kuroiwa T, Kopp JB, Nojima Y. Angiotensin II provokes podocyte injury in murine model of HIV-associated nephropathy. *Am J Physiol Renal Physiol.* 2007; 293:F1214–21. [PubMed: 17652372]
5. de P, Rodrigues SF, et al. *Life Sci.* 2006; 78:2280–5. [PubMed: 16337658]
6. Suzuki K, Han GD, Miyauchi N, et al. Angiotensin II type 1 and type 2 receptors play opposite roles in regulating the barrier function of kidney glomerular capillary wall. *Am J Pathol.* 2007; 170:1841–1853. [PubMed: 17525253]
7. Masaki H, Kurihara T, Yamaki A, Inomata N, Nozawa Y, Mori Y, Murasawa S, Kizima K, Maruyama K, Horiuchi M, Dzau VJ, Takahashi H, Iwasaka T, Inada M, Matsubara H. Cardiac-specific overexpression of angiotensin II AT2 receptor causes attenuated response to AT1 receptor-mediated pressor and chronotropic effects. *J Clin Invest.* 1998; 101:527–535. [PubMed: 9449684]
8. Inagami T, Eguchi S, Numaguchi K, Motley ED, Tang H, Matsumoto T, Yamakawa T. Cross-talk between angiotensin II receptors and the tyrosine kinases and phosphatases. *J Am Soc Nephrol.* 1999; 10 (suppl 11):57–61.
9. Nakajima M, Hutchinson HG, Fujinaga M, Hayashida W, Morishita R, Zhang L, Horiuchi M, Pratt RE, Dzau VJ. The angiotensin II type 2 (AT2) receptor antagonizes the growth effects of the AT1 receptor: gain-of-function study using gene transfer. *Proc Natl Acad Sci USA.* 1995; 92:10663–10667. [PubMed: 7479861]
10. Kambayashi Y, Bardhan S, Takahashi K, Tsuzuki S, Inui H, Hamakubo T, Inagami T. Molecular cloning of a novel angiotensin II receptor isoform involved in phosphotyrosine phosphatase inhibition. *J Biol Chem.* 1993; 268:24543–24546. [PubMed: 8227011]
11. Mukoyama M, Nakajima M, Horiuchi M, Sasamura H, Pratt RE, Dzau VJ. Expression cloning of type 2 angiotensin II receptor reveals a unique class of seven-transmembrane receptors. *J Biol Chem.* 1993; 268:24539–24542. [PubMed: 8227010]
12. Capponi AM. Distribution and signal transduction of angiotensin II AT1 and AT2 receptors. *Blood pressure, Supplement.* 1996; 2 :41–46. [PubMed: 8913539]
13. Akishita M, Iwai M, Wu L, Zhang L, Ouchi Y, Dzau VJ, et al. Inhibitory effect of angiotensin II type 2 receptor on coronary arterial remodeling after aortic banding in mice. *Circulation.* 2000; 102:1684–1689. [PubMed: 11015348]
14. Viswanathan M, Saavedra JM. Expression of angiotensin II AT2 receptors in the rat skin during experimental wound healing. *Peptides.* 1992; 13:783–786. [PubMed: 1437716]
15. Leung PS, Chan HC, Fu LX, Wong PY. Localization of angiotensin II receptor subtypes AT1 and AT2 in the pancreas of rodents. *J Endocrinol.* 1997; 153:269–274. [PubMed: 9166116]
16. Nora EH, Munzenmaier DH, Hansen-Smith FM, Lombard JH, Greene AS. Localization of the ANG II type 2 receptor in the microcirculation of skeletal muscle. *Am J Physiol.* 1998; 275:H1395–H1403. [PubMed: 9746490]
17. Allen AM, Zhuo J, Mendelsohn FA. Localization of angiotensin AT1 and AT2 receptors. *J Am Soc Nephrol.* 1999; 10:S23–29. [PubMed: 9892137]
18. Wolf G, Butzmann U, Wenzel UO. The renin-angiotensin system and progression of renal disease: from hemodynamics to cell biology. *Nephron Physiol.* 2003; 93:P3–P13. [PubMed: 12411725]
19. Reudelhuber TL. The continuing saga of the AT2 receptor: a case of the good, the bad, and the innocuous. *Hypertension.* 2005; 46:1261–1262. [PubMed: 16286568]
20. Timmermans PC, Wong AT, Chiu WF, Benfield Herblin P, Carini DJ, et al. Angiotensin II receptors and angiotensin II receptor antagonists. *Pharmacol Rev.* 1993; 45:205–251. [PubMed: 8372104]
21. Griendling KK, Lassegue B, Alexander RW. Angiotensin receptors and their therapeutic implications. *Annu Rev Pharmacol Toxicol.* 1996; 36:281–306. [PubMed: 8725391]
22. Miura S, Karnik SS. Ligand-independent signals from angiotensin II type 2 receptor induce apoptosis. *EMBO J.* 2000; 19:4026–4035. [PubMed: 10921883]
23. Miura S, Karnik SS, Saku K. Constitutively active homo-oligomeric angiotensin II type 2 receptor induces cell signaling independent of receptor conformation and ligand stimulation. *J Biol Chem.* 2005; 280:18237–18244. [PubMed: 15746093]

24. Jin XQ, Fukuda N, Su JZ, Lai YM, Suzuki R, Tahira Y, et al. Angiotensin II type 2 receptor gene transfer downregulates angiotensin II type 1a receptor in vascular smooth muscle cells. *Hypertension*. 2002; 39:1021–1027. [PubMed: 12019286]
25. Noda K, Feng YH, Liu XP, Saad Y, Husain A, Karnik SS. The active state of the AT1 angiotensin receptor is generated by angiotensin II induction. *Biochemistry*. 1996; 35:16435–16442. [PubMed: 8987975]
26. Ardaillou R, Chansel D. Synthesis and effects of active fragments of angiotensin II. *Kidney Int*. 1997; 52:1458–1468. [PubMed: 9407491]
27. Zini S, Fournie-Zaluski MC, Chauvel E, Roques BP, Corvol P, Llorens-Cortes C. Identification of metabolic pathways of brain angiotensin II and III using specific aminopeptidase inhibitors: Predominant role of angiotensin III in the control of vasopressin release. *Proc Natl Acad Sci USA*. 1996; 93:11968–11973. [PubMed: 8876246]
28. Terui J, Tamoto K, Sudo J. Proteinuric potentials of angiotensin II, [des-Asp¹]-angiotensin II, and [des-Asp¹,des-Arg²]-angiotensin II in rats. *Biol Pharm Bull*. 1994; 17:1516–1518. [PubMed: 7703976]
29. Ruiz-Ortega M, Lorenzo O, Egido J. Angiotensin III upregulates genes involved in kidney damage in cultured mesangial cells and renal interstitial fibroblasts. *Kidney Int*. 1998; 54:S41–S45.
30. Ruiz-Ortega M, Lorenzo O, Egido J. Angiotensin III increases MCP-1 and activates NF- κ B and AP-1 in cultured mesangial and mononuclear cells. *Kidney Int*. 2000; 57:2285–2298. [PubMed: 10844599]
31. Matsubara H. Pathophysiological role of angiotensin II type 2 receptor in cardiovascular and renal diseases. *Circ Res*. 1998; 83:1182–1191. [PubMed: 9851935]
32. Kopp JB, Klotman ME, Adler SH, Bruggeman LA, Dickie P, Marinos NJ, Eckhaus M, Bryant JL, Notkins AL, Klotman PE. Progressive glomerulosclerosis and enhanced renal accumulation of basement membrane components in mice transgenic for human immunodeficiency virus type 1 genes. *Proc Natl Acad Sci U S A*. 1992; 89:1577–81. [PubMed: 1542649]
33. Arora S, Husain M, Kumar D, Patni H, Pathak S, Mehrotra D, Reddy VK, Reddy LR, Salhan D, Yadav A, Mathieson PW, Saleem MA, Chander PN, Singhal PC. Human immunodeficiency virus downregulates podocyte apoE expression. *Am J Physiol Renal Physiol*. 2009; 297:F653–61. [PubMed: 19553347]
34. AbdAlla S, Lothar H, Quitterer U. AT1-receptor heterodimers show enhanced G-protein activation and altered receptor sequestration. *Nature*. 2000; 407:94–98. [PubMed: 10993080]
35. AbdAlla S, Lothar H, Abd El Tawaab A, Quitterer U. The angiotensin II AT2 receptor is an AT1 receptor antagonist. *J Biol Chem*. 2001; 276:39721–39726. [PubMed: 11507095]
36. Su JZ, Fukuda N, Jin XQ, Lai YM, Suzuki R, Tahira Y, et al. Effect of AT2 receptor on expression of AT1 and TGF-beta receptors in VSMCs from SHR. *Hypertension*. 2002; 40:853–858. [PubMed: 12468569]
37. Widdop RE, Jones ES, Hannan RE, Gaspari TA. Angiotensin AT2 receptors: cardiovascular hope or hype? *Br J Pharmacol*. 2003; 140:809–824. [PubMed: 14530223]
38. Mukoyama M, Horiuchi M, Nakajima M, Pratt RE, Dzau VJ. Characterization of a rat type 2 angiotensin II receptor stably expressed in 293 cells. *Mol Cell Endocrinol*. 1995; 112:61–68. [PubMed: 7589786]
39. Hein L, Meinel L, Pratt RE, Dzau VJ, Kobilka BK. Intracellular trafficking of angiotensin II and its AT1 and AT2 receptors: evidence for selective sorting of receptor and ligand. *Mol Endocrinol*. 1971; 11:1266–1277. [PubMed: 9259318]
40. Ciuffo GM, Viswanathan M, Seltzer AM, Tsutsumi K, Saavedra JM. Glomerular angiotensin II receptor subtypes during development of rat kidney. *Am J Physiol*. 1993; 265:F264–271. [PubMed: 8368335]
41. Shanmugam C, Llorens-Cortes C, Clauser E, Corvol P, Gasc JM. Expression of angiotensin II AT2 receptor mRNA during development of rat kidney and adrenal gland. *Am J Physiol*. 1995; 268:F922–F930. [PubMed: 7771520]
42. Ozono R, Wang ZQ, Moore AF, Inagami T, Siragy HM, Carey RM. Expression of the subtype 2 angiotensin (AT2) receptor protein in rat kidney. *Hypertension*. 1997; 30:1238–1246. [PubMed: 9369282]

43. Cao Z, Kelly DJ, Cox A, Casley D, Forbes JM, Martinello P, et al. Angiotensin type 2 receptor is expressed in the adult rat kidney and promotes cellular proliferation and apoptosis. *Kidney Int.* 2000; 58:2437–2451. [PubMed: 11115077]
44. Ruiz-Ortega M, Esteban V, Suzuki Y, Ruperez M, Mezzano S, Ardiles L, et al. Renal expression of angiotensin type 2 (AT2) receptors during kidney damage. *Kidney Int Suppl.* 2003:S21–S26. [PubMed: 12969123]
45. Armando I, Jezova M, Juorio AV, Terron JA, Falcon-Neri A, Semino-Mora C, et al. Estrogen upregulates renal angiotensin II AT(2) receptors. *Am J Physiol Renal Physiol.* 2002; 283:F934–943. [PubMed: 12372768]
46. Baiardi G, Macova M, Armando I, Ando H, Tyurmin D, Saavedra JM. Estrogen upregulates renal angiotensin II AT1 and AT2 receptors in the rat. *Regulatory Pept.* 2005; 124:7–17.
47. Cao Z, Bonnet F, Candido R, Nesteroff SP, Burns WC, Kawachi H, et al. Angiotensin type 2 receptor antagonism confers renal protection in a rat model of progressive renal injury. *J Am Soc Nephrol.* 2002; 13:1773–1787. [PubMed: 12089373]
48. Bautista R, Sanchez A, Hernandez J, Oyekan A, Escalante B. Angiotensin II type AT(2) receptor mRNA expression and renal vasodilatation are increased in renal failure. *Hypertension.* 2001; 38:669–673. [PubMed: 11566953]
49. Hashimoto N, Maeshima Y, Satoh M, Odawara M, Sugiyama H, Kashihara N, et al. Overexpression of angiotensin type 2 receptor ameliorates glomerular injury in a mouse remnant kidney model. *Am J Physiol Renal Physiol.* 2004; 286:F516–525. [PubMed: 14583437]
50. Tejera N, Gomez-Garre D, Lazaro A, Gallego-Delgado J, Alonso C, Blanco J, et al. Persistent proteinuria up-regulates angiotensin II type 2 receptor and induces apoptosis in proximal tubular cells. *Am J Pathol.* 2004; 164 :1817–1826. [PubMed: 15111328]
51. Vazquez E, Coronel I, Bautista R, Romo E, Villalon CM, Avila-Casado MC, et al. Angiotensin II-dependent induction of AT(2) receptor expression after renal ablation. *Am J Physiol Renal Physiol.* 2005; 288:F207–F213. [PubMed: 15367388]
52. Ma J, Nishimura H, Fogo A, Kon V, Inagami T, Ichikawa I. Accelerated fibrosis and collagen deposition develop in the renal interstitium of angiotensin type 2 receptor null mutant mice during ureteral obstruction. *Kidney Int.* 1998; 53:937–944. [PubMed: 9551401]
53. Morrissey JJ, Klahr S. Effect of AT2 receptor blockade on the pathogenesis of renal fibrosis. *Am J Physiol.* 1999; 276:F39–F45. [PubMed: 9887078]

High lights

Ang II has been demonstrated to play an important role for the progression of HIVAN. This effect of Ang II has been demonstrated to be mediated predominantly through AT1R. Since AT2R activation induces opposite action to AT1R activation, we hypothesized that AT2R up regulation during AT1R blockade may also be contributing to the AT1R blockade-induced attenuation of the progression of HIVAN. The present study indicates that AT2R modulates HIV-induced renal lesions in HIV transgenic mice.

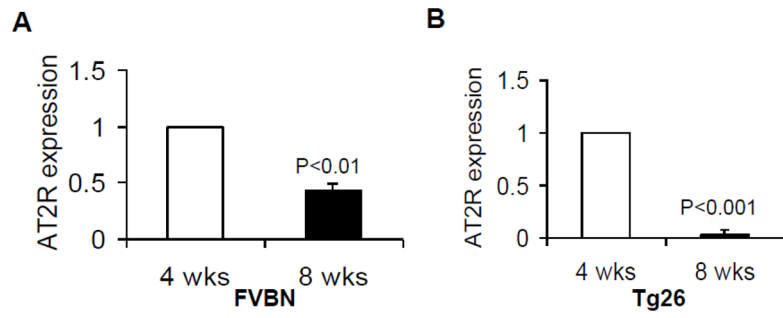


Fig. 1. Aging mice display reduction in renal tissue AT₂R expression

Total RNA was extracted from renal tissues of age and sex matched control (FVBN, 4 and 8 weeks old, n=3) and Tg26 (4 and 8 weeks old, n=3) mice. Renal tissue expression of AT2R was determined by real time PCR.

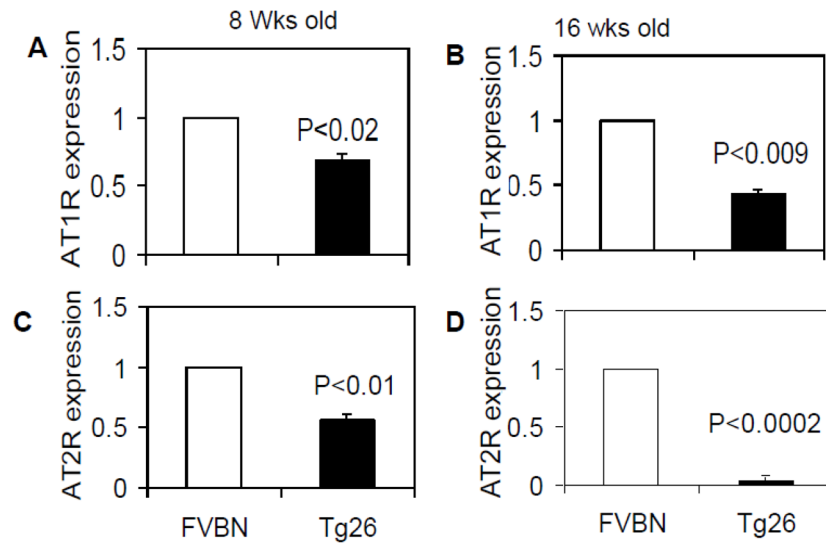


Fig. 2. Aging control and Tg26 mice display diminution of renal tissue expression AT₁R and AT₂R

Total RNA from renal tissues of eight and 16 weeks old control (FVBN, n=3) and Tg26 mice (n=3) was extracted. Renal tissue expression of AT₁R and AT₂R was assayed by real time PCR.

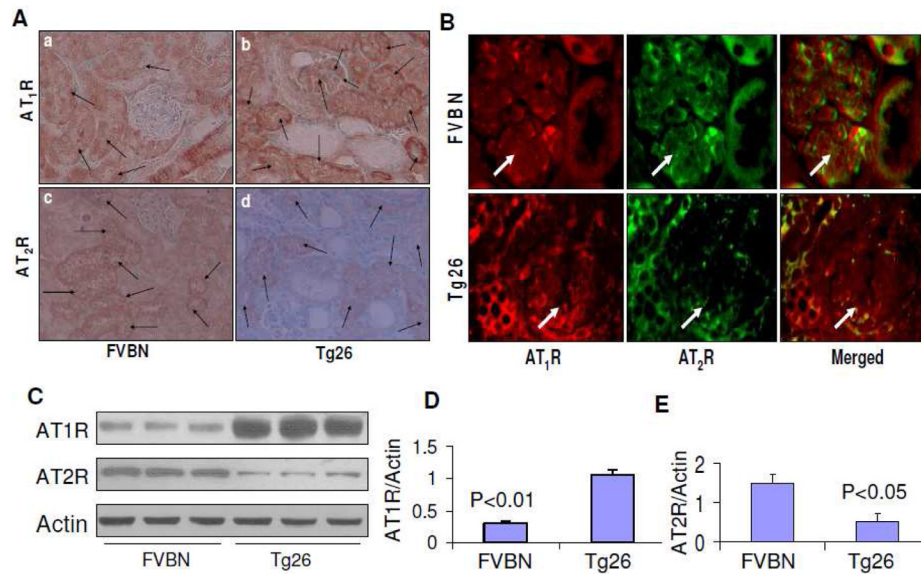


Fig. 3. Renal cell localization of AT₁R and AT₂R

A. Renal cortical sections of age and sex matched FVBN and Tg26 were immunolabeled for AT₁R and AT₂R.

a. A representative microphotograph of a renal cortical section from a control mouse is shown. Tubular cells displayed AT₁R expression as indicated by arrows.

b. A representative microphotograph from a cortical section of a Tg26 mouse is shown. Both glomerular and tubular cells showed expression of AT₁R (indicated by arrows).

c. A representative microphotograph of a renal cortical section from a control mouse is shown. Tubular cells show moderate labeling for AT₂R (indicated by arrows).

d. A representative microphotograph from a cortical section of a Tg26 mouse is shown. A few tubules show minimal immunolabeling for AT₂R (indicated by arrows).

B. Temporo-spatial relationship between AT₁R and AT₂R in glomerular and tubular cells in FVBN and Tg26 mice.

Renal cortical sections from FVBN and Tg26 mice were co-labeled for AT₁R and AT₂R and then examined under a fluorescence microscope. Representative microphotographs are shown. Glomeruli are indicated by white arrows.

C. Immunoblots from renal tissues from FVBN and Tg26 mice (n=3) were probed for AT₁R and AT₂R and actin. The upper lane displays renal tissue expression of AT₁R in FVBN and Tg26 mice. The middle panel shows renal tissue expression of AT₂R in FVBN and Tg26 mice. The lower panel shows renal tissue expression of actin under similar conditions.

D. Cumulative data in bar graphs showing renal tissue expression of AT₁R in FVBN and Tg26 mice (n=3).

E. Cumulative data in the form of a bar diagram displaying renal tissue expression of AT₂R in FVBN and Tg26 mice.

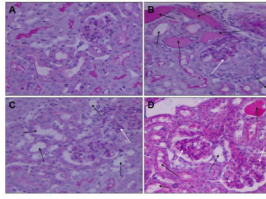


Fig. 4. Effect of AT₁R and AT₂R blockade of the progression of HIVAN AT1R

Tg26 mice in groups of four were administered either saline or telmisartan (AT₁R blocker, 300 µg/day), PD123319 (AT₂R blocker, 3 µg/day), telmisartan + PD123319 for two weeks. FVBN mice-receiving saline served as control for Tg26 mice receiving saline.

A. A representative microphotograph of a renal cortical section from a control mouse. Neither glomeruli nor tubules display any abnormality.

B. A representative microphotograph of a renal cortical section from a Tg26 mouse displaying proliferating glomerular epithelial cells and collapsed capillary loops (white arrow) and dilated tubules (black arrows).

C. A representative microphotograph of a renal cortical section from a mouse receiving telmisartan (AT1B) showing mild dilatation of tubules and mesangial cell proliferation (white arrow).

D. A representative microphotograph of a renal cortical section from a mouse receiving telmisartan (AT1B) + PD 123319 (AT2B) showing moderate tubular dilatation (black arrows) and significant mesangial cell proliferation (white arrows).

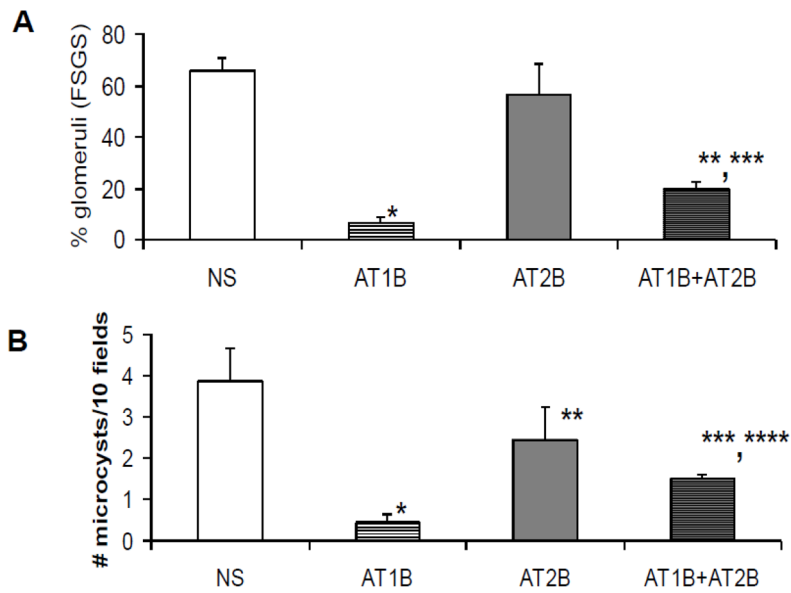


Fig. 5. Cumulative data on the effect of AT₁R and AT₂R blockade on severity of renal lesions Percentage of sclerosed glomeruli and number of microcyst were counted in Tg 26 mice receiving either saline, telmisartan (AT₁B), PD123319 (AT₂B), or telmisartan + PD123319 (AT₁+AT₂B) for two weeks.

A. Tg26 mice receiving telmisartan (AT₁B) displayed marked attenuation of the development of sclerosed glomeruli. Mice receiving POD123319 (AT₂B) did not display any reduction in percentage of sclerosed glomeruli; whereas, mice receiving both telmisartan and PD123319 displayed enhanced percentage of sclerosed glomeruli when compared to mice receiving telmisartan alone (AT₁B). *P<0.001 compared with NS; **P<0.05 compared with AT₁B; ***P<0.01 compared with AT₂B.

B. Tg26 mice receiving telmisartan (AT₁B) showed a reduction in number of microcysts. Mice receiving POD123319 (AT₂B) did not show any reduction in number of microcysts; however, mice receiving both telmisartan and PD123319 showed increased number of microcysts. when compared to mice receiving telmisartan alone (AT₁B). *P<0.001 compared with NS; **P<0.01 compared with AT₁B; ***P<0.01 compared with AT₁B; ****P<0.05 compared with AT₂B.

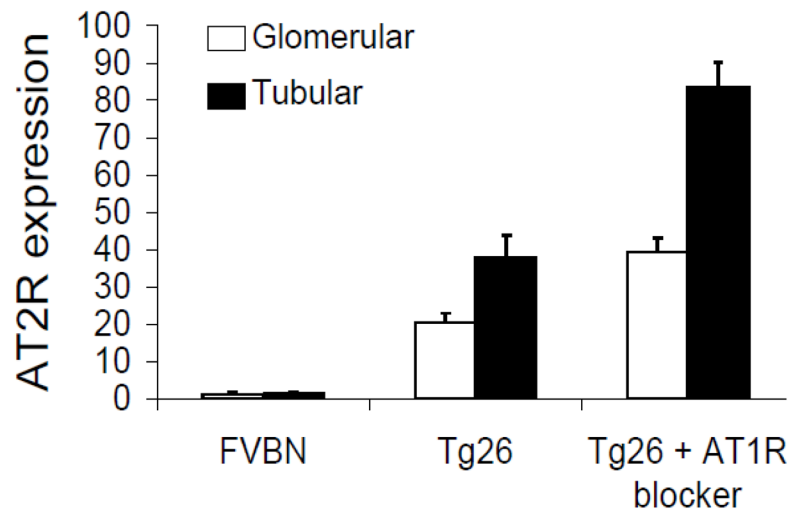


Fig. 6. Effect of AT₁ blockade on renal cell AT₂R expression

Renal cortical sections of control mice receiving normal saline, Tg26 mice receiving normal saline, and mice receiving telmisartan, (AT₁B) were immunolabeled for AT₂R. Percentage of glomeruli and tubules/field showing expression of AT₂R was recorded. Increased number of glomeruli and tubuli displayed expression of AT₂R in Tg26 mice. However, percentage of glomeruli and tubuli showing expression of AT₂R was two-fold higher in Tg26 mice receiving telmisartan when compared to Tg26 mice receiving normal saline.

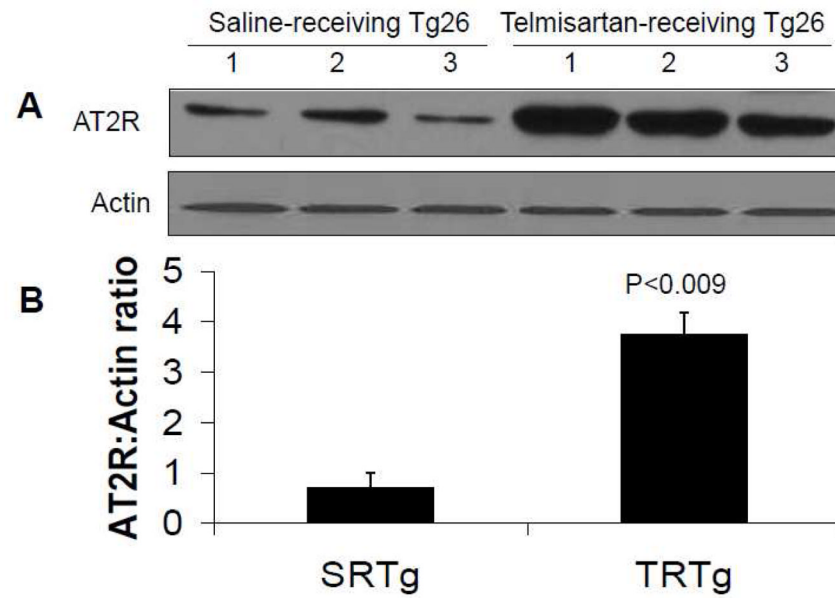


Fig. 7. Immunoblotting studies display enhanced renal tissue AT₂R expression in TRTgs
 Proteins were extracted from renal tissues of SRTgs (n=3) and TRTgs (n=3), Western blots were prepared and probed for AT₂R.

A. The upper lane represent renal tissue expression of AT₂R from SRTgs and TRTgs in triplicates. The lower panel represent actin content in each variable under the similar conditions.

B. Cumulative data in the form of bar diagram showing AT₂R expression by SRTgs and TRTgs.

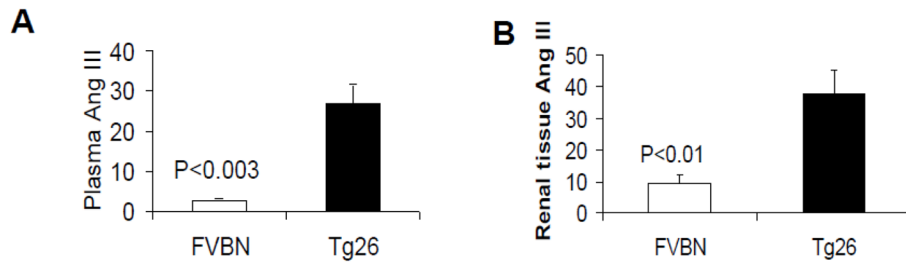


Fig. 8. Plasma and renal tissue concentrations of Ang III in control and Tg26 mice
Proteins were extracted from plasma (n=4) and renal tissue (n=4) age and sex matched four control and four Tg26 mice. Ang III concentration in lysates of plasma and renal tissues was measured by Ang III ELISA kit.

Table 1

Effect of AT1 and AT2 blockers on blood pressure of Tg26 mice

	Systolic (Mean)	Diastolic (Mean)
Normal saline	143.0 ± 2.1 *	109.1 ± 1.8 *
AT1 blocker	130.5 ± 2.5	100.2 ± 1.4
AT1 + AT2 blocker	129.8 ± 1.5	100.1 ± 1.3

* P<0.01 compared to respective variables